Anaerobic Digestion of Aqueous Pyrolysis Liquid in ADM1

Dheeraj Raya[1] Nirmal Ghimire[1] Gudny Øyre Flatabø[1,2] Wenche Hennie Bergland[1]

[1]Department of Process, Energy and Environmental Technology, University of South-Eastern Norway
[2]Scanship AS, Nedre Langgate 19, 3126, Tønsberg, Norway
rayadheeraj@gmail.com, nirmal.ghimire@usn.no, gudny.flatabo@scanship.no, wenche.bergland@usn.no

Abstract

Aqueous pyrolysis liquid (APL) is formed from pyrolysis of lignocellulosic biomass and is considered as a possible feed for anaerobic digestion (AD). APL is known to contain many components that can have a negative impact on the AD process. In this study, APL is fed into experimental AD batch reactors and modelled as a substrate using the Anaerobic Digestion Model No. 1 (ADM1), extended by addition of the inhibitors phenol, furfural, and 5-hydroxymethylfurfural (HMF). Simulation performed with the extended ADM1 has a better ability to predict the behavior of APL than the standard ADM1. Reducing the inhibition constants and startup concentration of active biomass during simulation of APL at high organic load resulted in improved fit with experimental results, but these inhibitors alone cannot explain the reduced methane production rate at high organic load.

Keywords: Anaerobic Digestion, Lignocellulosic biomass, Aqueous Pyrolysis Liquid, phenol, furfural, HMF, inhibition, ADM1

1 Introduction

Dry lignocellulosic biomasses are abundant in nature and can be harvested sustainably (Feng and Lin, 2017). Using thermochemical and biochemical processes, we can convert such biomasses into energy, either for heat or electricity generation or even as a transport fuel such as biomethane (Pang, 2019). Pyrolysis, a thermochemical process used for dry biomasses, produces value added products such as biochar, syngas, bio-oil, and aqueous pyrolysis liquid (APL) (McNamara et al., 2016).

APL has a high organic content, showing potential for conversion to biogas through anaerobic digestion (AD) (Hübner and Mumme, 2015). However, APL is a complicated mixture – known to contain more than 400 chemical compounds – many of which can have a negative impact on the AD process (Seyedi et al., 2019). Compounds such as phenols, furfural, and 5-hydroxymethylfurfural (HMF) present in APL are known to be inhibitory to AD (Torri and Fabbri, 2014).

Anaerobic digestion, a biochemical process mostly used for treating wastewater, produces biogas that can be upgraded to biomethane. Methanogenesis is the final step that converts acetate (acetoclastic) and hydrogen (hydrogenotrophic) into methane and is also often a rate limiting step in the AD process. APL concentration of 2-4 g COD/L (COD: chemical oxygen demand) has been previously reported to completely inhibit the AD process (Seyedi et al., 2019). Constituents of APL such as phenol, furfural and HMF inhibits the methanogenesis process completely at concentration of 2.5 g/L (Olguin-Lora et al., 2003), 2 g/L (Ghasimi et al., 2016) and 2 g/L (Ghasimi et al., 2016) respectively.

However, microorganisms present in AD are known to thrive in the presence of inhibitory compounds, managing to degrade them during the AD process. Phenol, a weak acid, is broken down to the intermediate benzoate, before it is degraded completely to acetate and hydrogen (Fezzani and Ben Cheikh, 2009). Similarly, furfural and HMF also breaks down anaerobically producing acetate as the final product (Zhang et al., 2012).

The Anaerobic Digestion Model No.1 (ADM1) (Batstone et al., 2002), developed by the International Water Association (IWA), has been widely used by the scientific community for evaluating the performance of AD processes under different substrate and reactor configurations. However, the model has been limited to only major AD processes to make it simpler and easier for modification in the future as per need. Complex substrates such as APL are gaining interest and the constituent phenol is already implemented in ADM1 (Fezzani and Ben Cheikh, 2009), but modifications are needed to study the inhibition caused by the APL constituents furfural and HMF.

Through this study, we aim to better understand the effects of inhibitory compounds present in APL, represented by phenols, furfural and HMF, to predict and simulate the dynamic behavior of AD of APL using ADM1.

2 Materials and Methods

Batch anaerobic reactors, fed APL and run mesophilic, are compared with ADM1 extended with the inhibitor's phenol, furfural, and HMF, known to be present in APL.

2.1 Analytical methods

Total COD (tCOD), soluble COD (sCOD), volatile fatty acids (acetic acid, propionic acid, butyric acid, iso-butyric acid), pH, and ammonium content were analyzed as described in Bergland et al., (2015).

2.2 Material Characterization

2.2.1 APL

APL was obtained from pyrolysis of commercial softwood pellets (Norway spruce and Scots pine 60/40 per volume, Hallingdal Trepellets AS) at 600˚C, using the Biogreen® technology. The pyrolysis liquid was condensed from syngas cooled to 5-8 ˚C, and the APL provided was the top phase decanted after settling by gravity for two weeks in a cool environment.

APL had a tCOD and sCOD of 456 and 428 g/L and contained 75.83 and 5.33 g/L of acetic acid and propionic acid, respectively. APL had a low pH of 2.46.

2.2.2 Inoculum

Inoculum was obtained from Lindum AD plant in Drammen, Norway, a mesophilic process with an installed thermal hydrolysis step prior to AD. The plant treats sewage sludge from surrounding municipalities (about 90% of total volatile solids) and food waste from industry. The inoculum was collected from the effluent stream of the reactor and had a pH of 7.97, total solids (TS) of 16.78 g/L, volatile solids (VS) of 13.14 g/L, and total ammonium nitrogen (TAN) of 486 mg/L.

2.3 Batch Reactor Set up

Anaerobic biogas potential tests were performed in the Automatic Methane Potential Test System II (AMPTS II, Bioprocess Control® Sweden AD, Lund, Sweden 2017). It is used to determine the methane production from any biodegradable material. The experimental procedure can be found in Ghimire et al. (2020). Batch reactors of 500 mL were used with 300 mL of inoculum, and APL was added to have an organic load (OL) of 1.2 and 2.4 g COD APL per litre of inoculum. Additional blank reactors included only inoculum and was used to consider the background methane production. All the reactors were run at 35 ℃ for 54 days with 2 parallels for each test.

2.4 Modelling and Simulation

The original ADM1 was extended by the addition of phenol, furfural and HMF as inhibitory compounds (extended ADM1) (Figure 1). The inclusion of these inhibitory compounds requires the addition of 8 processes (Table 1).

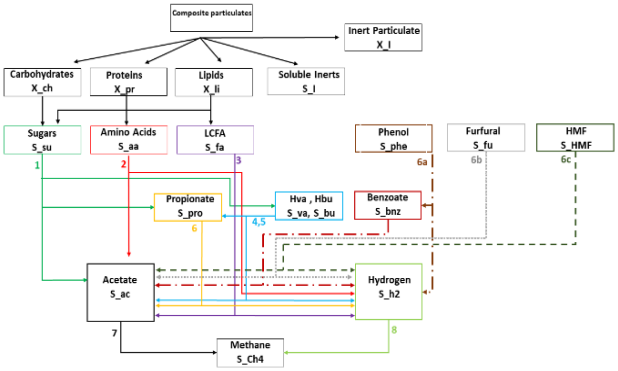

Figure 1. A brief schematic of the extended ADM1.

Table 1. Biochemical stochiometric coefficients and kinetic rate equations for compounds (only additional processes and compounds to standard ADM1 are shown).

	j	6a	6a-1	6b	6c	7	8	9	10	11	22a	22b	22c	22d	22	
	Component ->i	S_phe	S_bnz	S_fu	S_HMF	S_ac	S_h2	S_ch4	S_IC	S_IN	X_Phe	X_bnz	X_fu	X_HMF	X_ac	
	Process	Uptake of Phenol	Uptake of Benzoate	Uptake of Furfural	Uptake of HMF	Uptake of Acetate	Decay of X_phe	Decay of X_bnz	Decay of X_fu	Decay of X_HMF	Decay of X_ac						Rate (ρ_j, kgCOD/m^3*d)
Total Phenol (kgCOD/m^3)																	
Total Benzoate (kgCOD/m^3)		f_bnz_phe*(1-Y_phe)	-1														
Total Furfural (kgCOD/m^3)				-1													
Total HMF (kgCOD/m^3)					-1												
Total Acetate (kgCOD/m^3)			f_ac_bnz*(1-Y_bnz)	f_ac_fu*(1-Y_fu)	f_ac_HMF*(1-Y_HMF)	-1											
Hydrogen gas (kgCOD/m^3)		f_h2_phe*(1-Y_phe)	f_h2_bnz*(1-Y_bnz)	f_h2_fu*(1-Y_fu)	f_ac_HMF*(1-Y_HMF)												
Methane gas (kgCOD/m^3)						(1-Y_ac)											
Inorganic carbon (kmoleC/m^3)		-sum(C_i*vi_6a)	sum(C_i*vi_6a-1)	sum(C_i*vi_6b)	sum(C_i*vi_6c)	- sum(C_i*vi_7)											
Inorganic nitrogen (kmoleC/m^3)		-(Y_phe)*N_bac	-(Y_bnz)*N_bac	-(Y_fu)*N_bac	-(Y_HMF)*N_bac	-(Y_ac)*N_bac											
Phenol degraders (kgCOD/m^3)			Y_phe				-1										
Benzoate degraders (kgCOD/m^3)				Y_bnz				-1									
Furfural degraders (kgCOD/m^3)					Y_fu				-1								
HMF degraders (kgCOD/m^3)						Y_HMF				-1							
Acetate degraders (khCOD/m^3)							Y_ac									-1	
		km_phe*(S_phe/(Ks+S_phe))*X_phe*I_1	km_bnz*(S_bnz/(Ks+S_bnz))*X_bnz*I_1*I_h2_bnz	km_fu*(S_fu/(Ks+S_fu))*X_fu*I_1	km_HMF*(S_HMF/(Ks+S_HMF))*X_HMF*I_1	km_ac*(S_ac/(Ks+S_ac))*X_ac*I_2	kdec_X_phe*X_phe	kdec_X_bnz*X_bnz	kdec_X_fu*X_fu	kdec_X_HMF*X_HMF	kdec_X_ac*X_ac					-1	Inhibition: I_1=I_pH*I_NH_lim; I_2=I_pH*I_NH_lim*I_NH3_xac*I_phe_ac*I_fu_ac*I_HMF_ac

Each conversion process was implemented by several kinetic expressions that describe the conversion processes in terms of rate constants and substrate concentration. The conversion of inhibitory compounds to their respective products was described using Monod's growth kinetic equation. Endogenous decay of the biomass degrading the inhibitory compounds was modelled using first order kinetics, and dead biomass was maintained as composite particulates as in the original ADM1.

The detailed stoichiometry of all the processes and rate equations used are presented (Table 1) with their respective values (Table 2). The uptake of acetate in the extended ADM1 was modified by addition of inhibition from phenols, furfural and HMF as shown by process 7 in Table 1. Inhibition by phenol, furfural and HMF was modelled using a non-competitive inhibition function (1) (Batstone et al., 2002).

$$I = \frac{1}{1+\frac{S}{K_i}} \quad (1)$$

I = Inhibition, S = concentration of substrate in kg COD/m^3, and K_i = inhibition constant (concentration of substrate that inhibits the activity of the microorganisms by 50%).

Phenol is a weak acid and both phenol and benzoate contribute to pH changes. The charge balance equation used in the standard ADM1 (Batstone et al., 2002) was extended to include the contributions from phenol and benzoate (2).

$$S_{H^+} - S_{OH^-} = S_{HCO_3^-} + \frac{S_{ac^-}}{64} + \frac{S_{pro^-}}{112} + \frac{S_{bu^-}}{160} + \frac{S_{va^-}}{208} + \frac{S_{phe^-}}{224} + \frac{S_{bnz^-}}{240} + S_{An^+} - S_{cat^+} - S_{NH_4^+} \quad (2)$$

Where S_{phe^-} and S_{bnz^-} are phenol (3) and benzoate ion concentration (4), implemented in ADM1 as described by Batstone et al. (2002).

$$S_{phe^-} - \frac{K_{a,phe} \times S_{phe}}{K_{a,phe} + S_{H^+}} = 0 \quad (3)$$

Where $K_{a,phe}$ (phenolic acid dissociation constant) is 1×10^{-10}(Sharma and Kaminski, 2012).

$$S_{bnz^-} - \frac{K_{a,bnz} \times S_{bnz}}{K_{a,bnz} + S_{H^+}} = 0 \quad (4)$$

Where the $K_{a,bnz}$ (benzoic acid dissociation constant) is 6.3×10^{-5} (*Ionization Constants of Organic Acids*, n.d.)

Table 2. Kinetics parameters and their respective value used for degradation of phenol, furfural and HMF

Parameter	*Description*	*Unit*	*Phenol*	*Benzoate*	*Furfural*	*HMF*	*Value*
C	Carbon content in compound	KmoleC/kg COD	0.391[a]	0.0343[a]	5/160[e]	6/192[e]	-
Km	Maximum uptake rate	d-1	15[a]	8[a]	10[c]	10[c]	-
Ks	Half saturation constant for uptake	kg CODs/m3	30[a]	15.5[a]	10[c]	10[c]	-
Kdec	Decay rate for biomass	d-1	0.02	0.02	0.02[d]	0.01[c]	-
Y	Yield of biomass on uptake	kg CODx/kg CODs	0.01[a]	0.013[a]	0.08[d]	0.1[c]	-
Ki	Inhibition on methanogens from compound	kg CODs/m3	1.12[a]	-	2.105[e]	2.05[e]	-
Ki_bnz_h2	Inhibition on benzoate degraders by hydrogen	kg CODs/m3	-	9.50E-05[b]	-	-	-
X	Concentration of biomass	kg CODx/m3	0.21	0.24	0.12	0.18	-
f_bnz_phe	Yield of benzoate from phenol		-	-	-	-	0.87[a]
f_h2_phe	Yield of hydrogen from phenol		-	-	-	-	0.13[a]
f_ac_bnz	Yield of acetate from benzoate		-	-	-	-	0.51[a]
f_h2_bnz	Yield of hydrogen from benzoate		-	-	-	-	0.49[a]
f_ac_fu	Yield of acetate from furfural		-	-	-	-	0.8[d]
f_h2_fu	Yield of hydrogen from furfural		-	-	-	-	0.2[d]
f_ac_HMF	Yield of acetate from HMF		-	-	-	-	0.88[c]
f_h2_HMF	Yield of hydrogen from HMF		-	-	-	-	0.12[c]

[a] (Fezzani and Ben Cheikh 2009)
[b] (Elshahed et al. 2001)
[c] (Liu et al. 2017)
[d] (Brune, Schoberth, and Sahm 1983)
[e] calculated

2.4.1 APL characteristics

APL concentrations implemented in ADM1 (Table 3) were measured based on APL characteristics. Phenol, furfural and HMF concentrations are not known and were from reporting APL from birch bark (hardwood) pyrolysed at 600 °C.

Table 3. APL composition used for simulations.

Parameters	*Value*
Acetic acid (g/L)	75.832[f]
Propionic acid (g/L)	5.33 [f]
Phenol (g/L)	25[g]
Furfural (g/L)	10[h]
HMF (g/L)	7 [h]
Soluble Inorganic Nitrogen (kmole/m^3)	0.025[e]
X_C	Calculated

Around 50 % of the APL COD is unknown and was added as complex particulate (X_C) already present in the ADM1.

2.4.2 Determination of inhibition constant for furfural and HMF

Prior knowledge of the inhibition constant for furfural and HMF (1) required for modelling the inhibition effect is not found in the literature. Experimental results of specific methanogenic activity (SMA) from Ghasimi et al. (2016) is used to determine the IC_{50} value that can be used as inhibition constant K_i (1). Thus, inhibition constant values are calculated graphically to obtain the IC_{50} value, the concentration of substrate at which 50% inhibition occurs (Figure 2).

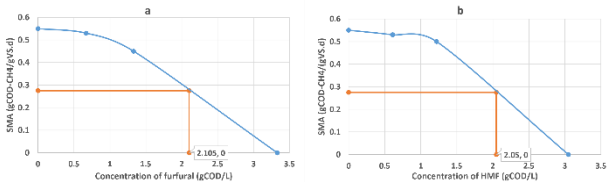

Figure 2. IC_{50} value determination using graphical method for a: furfural and b: HMF. Based on SMA activity from Ghasimi et al. (2016).

2.4.3 Simulation strategy

To evaluate the extended model, the simulation was performed based on three strategies:

1. Vary the concentration of inhibitory compounds to evaluate the effect (Table 4).
2. Vary the inhibition constant to evaluate the sensitivity in the model (Table 5).
3. Vary the startup active biomass concentration of inhibitory compounds degraders. Both sufficient and low startup concentration of biomass (X_low=X×0.1) were tested.

Table 4. Concentration of inhibitory compounds in APL used in simulations of AD of APL at OL of 1.2 and 2.4 g COD/L.

Inhibitory compounds	*Sim-base*	*Sim-inhib-low*	*Sim-inhib-avg*	*Sim-inhib-high*
Phenol (g/L)	25	5	25	40
Furfural (g/L)	10	5	25	40
HMF (g/L)	7	5	25	40

Table 5. Inhibition constant used in simulations of AD of APL at OL of 2.4 g COD/L.

Inhibition constant	*Sim-base*	*Sim-Ki_low_1*	*Sim-Ki_low_2*	*Sim-Ki_low_3*
KI_fu (kg COD/m^3)	2.10	0.84	0.21	0.11
KI_HMF (kg COD/m^3)	2.05	0.82	0.21	0.10
KI_phe (kg COD/m^3)	1.12	0.45	0.11	0.06

3 Results and Discussion

3.1 Experimental Results

The methane production rate (Figure 3) was low for APL with OL of 2.4 g COD/L (APL2.4) and was same as Blank (only inoculum) till day 2, whereas APL with OL of 1.2 g COD/L (APL1.2) had a gradual methane production until day 20 with no lag phase. Unpublished results during batch AD tests of the same APL gave increased lag phase when the organic load was higher than 2 g COD/L and total inhibition at OL of 3 g COD/L.

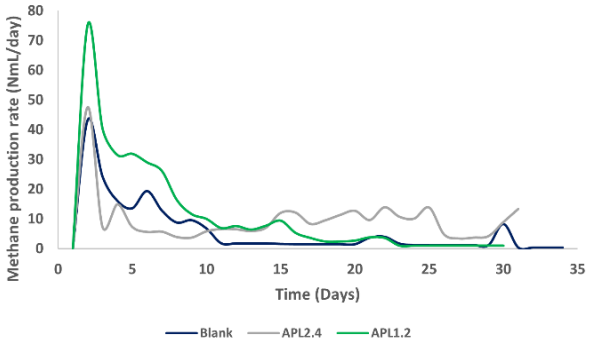

Figure 3. Methane production rate from batch test of APL at organic load of 1.2 and 2.4 g COD/L referred to as

[f] Measured
[g] (Yu et al. 2020)
[h] (Torri and Fabbri 2014)

APL1.2 and APL2.4, respectively, along with results from blank (only inoculum).

3.2 Simulation results

3.2.1 Simulation of APL

Simulation of APL1.2 (sim1.2) by standard ADM1 and extended ADM1 shows a good fit to the experimental results (Figure 4), however, both standard and extended ADM1 was not able to follow the trend of methane production rate at high OL (sim2.4).

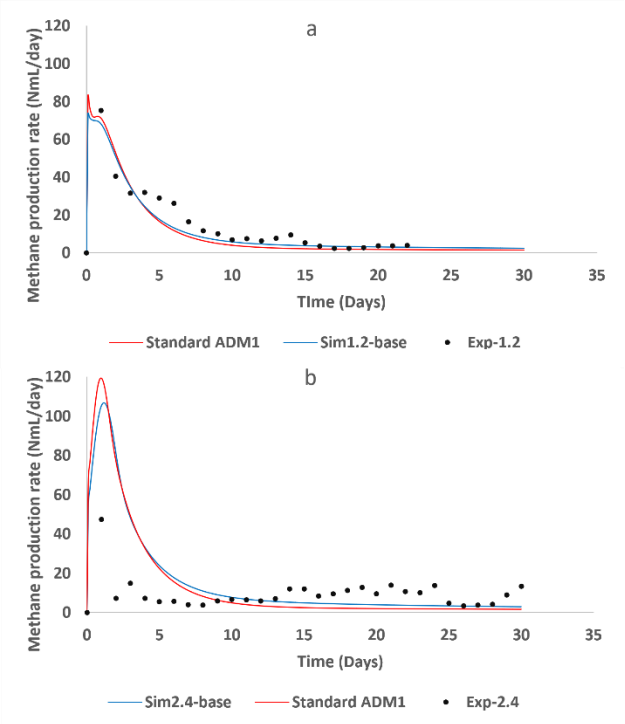

Figure 4. Simulated methane production rate using standard ADM1 (red line), extended ADM1 model (blue line) and experimental results (black dots) for APL a: at organic load of 1.2 g COD/L (Sim1.2-base) b: at organic load of 2.4 g COD/L (Sim2.4-base).

3.2.2 Simulation with varying inhibitory compound concentration

Simulations performed with varying concentrations of inhibitory compounds revealed only a small effect on the methane production rate for APL at low OL of 1.2 g COD/L (Figure 5). However, the effect from high inhibitor concentrations at OL of 2.4 g COD/L of APL was more pronounced. High OL and thereby high concentration of inhibitory compounds resulted in inhibition and a lower maximum methane production rate.

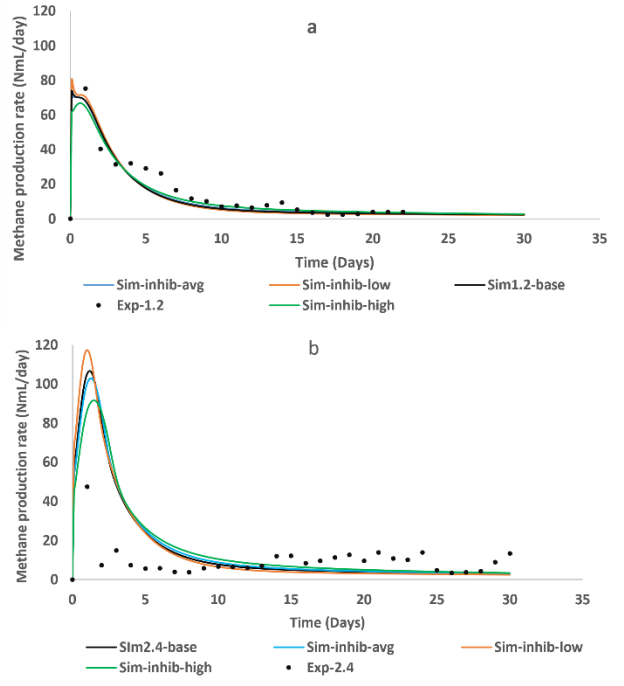

Figure 5. Simulation with varying concentration of inhibitory compounds (Table 5). a: simulated methane production rate for APL1.2 with experimental results (black dots) b: simulated methane production rate for APL2.4 with experimental results (black dots).

The inhibition by the individual inhibitory compounds increased with an increase in concentration (Figure 6). Phenol causes the highest inhibition effect on the methanogens. The total effect from the inhibitors can however not explain the low fit between the simulations and the experiment with OL of 2.4 g COD APL/L (Figure 5).

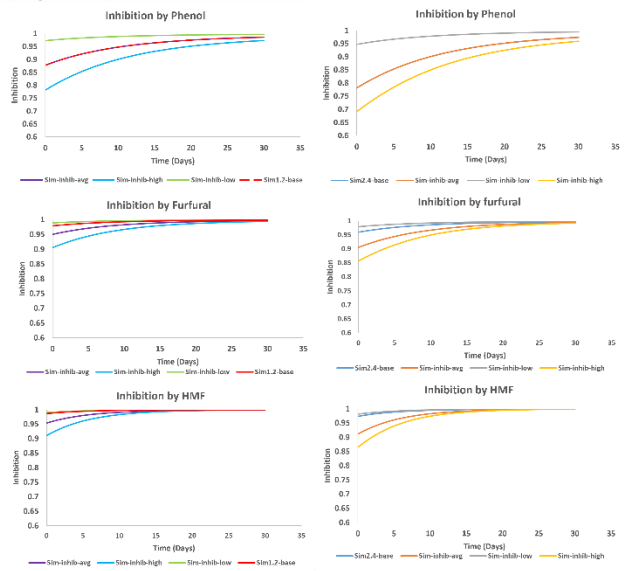

Figure 6. Inhibition by inhibitory compounds on methanogens. 1 is no inhibition at all and 0 is full inhibition. a: simulated inhibition for APL OL of 1.2 g COD/L b: simulated inhibition for APL OL of 2.4 g COD/L.

3.2.3 Simulation with varying inhibition constant and low biomass concentration of inhibitory compound degraders

Reducing the estimated inhibition constants (Table 5) resulted in a maximum methane production rate that decreased drastically (Figure 7). This is however not based on real inhibition constants but rather reveals the high degree of sensitivity towards a change in the inhibition constant. The concentration of active initial biomass degrading the individual inhibitory compounds is not known and reducing these concentrations (Figure 7) also reveals an effect further reducing the gap between experiment and simulated methane production rate at OL 2.4 g COD APL/L.

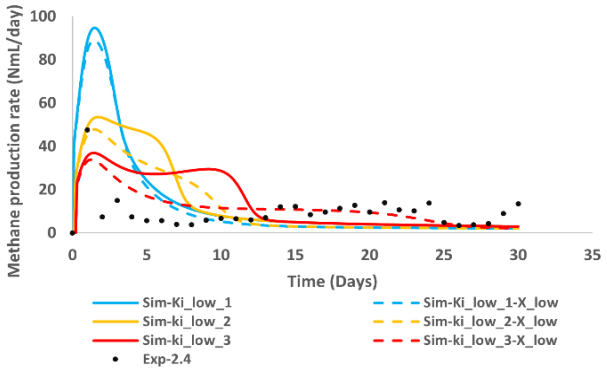

Figure 7. Simulated methane production rate with low initial startup concentration of inhibitory compounds degrading biomass (Sim-Ki_low_3-X_low, Sim-Ki_low_2-X_low, and Sim-Ki_low_1-X_low) represented by dashed lines and simulation with only change in inhibition constant for inhibitory compounds represented by lines. Experiment with OL 2.4 g COD APL/L (black dots).

Even though the inhibition constant used in Sim-Ki_low_3-X_low was low, it can be justified that there are a lot of unknown compounds in APL that have potential to inhibit the methanogenesis. Compounds such as chlorinated alkenes and alkanes, nitros and nitriles are known to severely inhibit the methanogenesis even at low concentrations (Blum and Speece, 1991). Thus, there is the possibility that the inhibition seen using the lowest inhibition constant (Sim-Ki_low_3 and Sim-Ki_low_3-X_low in Figure 7) could also be observed if further inhibitory compounds are added to the model, such as ketones, polyaromatic hydrocarbons and esters – which are also known to be present in APL and known to inhibit methanogenesis (Blum and Speece, 1991). Microorganism can however also be adapted to inhibitors (Badshah, 2012;Wen, 2020) suggesting lower inhibition over time in continuous AD reactors.

4 Conclusion

The effect of the inhibitors furfural, HMF, and phenols present in APL using ADM1 reveals a high sensitivity of the inhibition constant (made from 50% inhibition of the methanogens). When using realistic values for the inhibition constants and concentrations of inhibitory compounds, the reduced methane production rate at high organic load of APL cannot be explained by furfural, HMF, and phenols alone in batch AD. APL contains several known and unknown compounds and it is suggested to study more of these to find the combined inhibitory effect.

References

M. Badshah. Evaluation of process parameters and treatments of different raw materials for biogas production (PhD Thesis), Lund University, 2012. https://lup.lub.lu.se/record/3130472

D. J. Batstone, J. Keller, I. Angelidaki, S. V. Kalyuzhnyi, S. G. Pavlostathis, A. Rozzi, W. T. M. Sanders, H. Siegrist, and V. A. Vavilin. The IWA Anaerobic Digestion Model No 1 (ADM1). *Water Science and Technology*, *45*(10), 65–73, 2002. https://doi.org/10.2166/wst.2002.0292

W. H. Bergland, C. Dinamarca, M. Toradzadegan, A. S. R. Nordgård, I. Bakke, and R. Bakke. High rate manure supernatant digestion. *Water Research*, *76*, 1–9, 2015. https://doi.org/10.1016/j.watres.2015.02.051

D. J. Blum, and R. E. Speece. *A database of chemical toxicity to environmental bacteria and its use in interspecies comparisons and correlations*. *63*(3), 198–207, 1991.

G. Brune, S. M. Schoberth, and H. Sahm. Growth of a Strictly Anaerobic Bacterium on Furfural (2-Furaldehyde). *Applied and Environmental Microbiology*, *46*(5), 1187–1192, 1983. https://doi.org/10.1128/AEM.46.5.1187-1192.1983

M. S. Elshahed, V. K. Bhupathiraju, N. Q. Wofford, M. A. Nanny, and M. J. McInerney. Metabolism of Benzoate, Cyclohex-1-ene Carboxylate, and Cyclohexane Carboxylate by "Syntrophus aciditrophicus" Strain SB in Syntrophic Association with H2-Using Microorganisms. *Applied and Environmental Microbiology*, *67*(4), 1728–1738, 2001. https://doi.org/10.1128/AEM.67.4.1728-1738.2001

Q. Feng, and Y. Lin. Integrated processes of anaerobic digestion and pyrolysis for higher bioenergy recovery from lignocellulosic biomass: A brief review. *Renewable and Sustainable Energy Reviews*, *77*, 1272–1287, 2017. https://doi.org/10.1016/j.rser.2017.03.022

B. Fezzani, and R. Ben Cheikh. Extension of the anaerobic digestion model No. 1 (ADM1) to include phenol compounds biodegradation processes for simulating the anaerobic co-digestion of olive mill wastes at mesophilic temperature. *Journal of Hazardous Materials*, *172*(2–3), 1430–1438, 2009. https://doi.org/10.1016/j.jhazmat.2009.08.017

D. S. M. Ghasimi, K. Aboudi, M. de Kreuk, M. H. Zandvoort, and J. B. van Lier. Impact of lignocellulosic-waste intermediates on hydrolysis and methanogenesis under thermophilic and mesophilic conditions. *Chemical Engineering Journal*, *295*, 181–191, 2016. https://doi.org/10.1016/j.cej.2016.03.045

N. Ghimire, R. Bakke, and W. H. Bergland. Thermophilic Methane Production from Hydrothermally Pretreated

Norway Spruce (Picea abies). *Applied Sciences*, *10*(14), 4989, 2020. https://doi.org/10.3390/app10144989

T. Hübner, and J. Mumme. Integration of pyrolysis and anaerobic digestion – Use of aqueous liquor from digestate pyrolysis for biogas production. *Bioresource Technology*, *183*, 86–92, 2015. https://doi.org/10.1016/j.biortech.2015.02.037

Ionization Constants of Organic Acids. (n.d.). Retrieved April 21, 2021, from https://www2.chemistry.msu.edu/faculty/reusch/VirtTxtJml/acidity2.htm

B. Liu, V. A. Ngo, M. Terashima, and H. Yasui. Anaerobic treatment of hydrothermally solubilised sugarcane bagasse and its kinetic modelling. *Bioresource Technology*, *234*, 253–263, 2017. https://doi.org/10.1016/j.biortech.2017.03.024

P. J. McNamara, J. D. Koch, Z. Liu, and D. H. Zitomer. Pyrolysis of Dried Wastewater Biosolids Can Be Energy Positive. *Water Environment Research*, *88*(9), 804–810, 2016. https://doi.org/10.2175/106143016X14609975747441

P. Olguin-Lora, L. Puig-Grajales, and E. Razo-Flores. Inhibition of the acetoclastic methanogenic activity by phenol and *alkyl* phenols. *Environmental Technology*, *24*(8), 999–1006, 2003. https://doi.org/10.1080/09593330309385638

S. Pang. Advances in thermochemical conversion of woody biomass to energy, fuels and chemicals. *Biotechnology Advances*, *37*(4), 589–597, 2019. https://doi.org/10.1016/j.biotechadv.2018.11.004

S. Seyedi, K. Venkiteshwaran, and D. Zitomer. Toxicity of Various Pyrolysis Liquids From Biosolids on Methane Production Yield. *Frontiers in Energy Research*, *7*, 5, 2019. https://doi.org/10.3389/fenrg.2019.00005

I. Sharma and G. A. Kaminski. Calculating pKa values for substituted phenols and hydration energies for other compounds with the first-order Fuzzy-Border continuum solvation model. *Journal of Computational Chemistry*, *33*(30), 2388–2399. PubMed, 2012. https://doi.org/10.1002/jcc.23074

C. Torri, and D. Fabbri. Biochar enables anaerobic digestion of aqueous phase from intermediate pyrolysis of biomass. *Bioresource Technology*, *172*, 335–341, 2014. https://doi.org/10.1016/j.biortech.2014.09.021

C. Wen, C. M. Moreira, L. Rehmann, and F. Berruti. Feasibility of anaerobic digestion as a treatment for the aqueous pyrolysis condensate (APC) of birch bark. *Bioresource Technology*, *307*, 123199, 2020. https://doi.org/10.1016/j.biortech.2020.123199

X. Yu, C. Zhang, L. Qiu, Y. Yao, G. Sun, and X. Guo. Anaerobic digestion of swine manure using aqueous pyrolysis liquid as an additive. *Renewable Energy*, *147*, 2484–2493, 2020. https://doi.org/10.1016/j.renene.2019.10.096

Y. Zhang, B. Han, and T. C. Ezeji. Biotransformation of furfural and 5-hydroxymethyl furfural (HMF) by Clostridium acetobutylicum ATCC 824 during butanol fermentation. *New Biotechnology*, *29*(3), 345–351, 2012. https://doi.org/10.1016/j.nbt.2011.09.001